



Highly efficient near-infrared quantum cutting in Ce³⁺/Yb³⁺ co-doped chalcohalide glasses

Bing Gao, Qiqi Yan, Yu Tong, Xianghua Zhang, Hongli Ma, Jean-Luc Adam, Jing Ren, Guorong Chen

► To cite this version:

Bing Gao, Qiqi Yan, Yu Tong, Xianghua Zhang, Hongli Ma, et al.. Highly efficient near-infrared quantum cutting in Ce³⁺/Yb³⁺ co-doped chalcohalide glasses. *Journal of Luminescence*, 2013, 143, pp.181-184. <10.1016/j.jlumin.2013.04.015>. <hal-00859852>

HAL Id: hal-00859852

<https://hal.science/hal-00859852v1>

Submitted on 9 Oct 2013

HAL is a multi-disciplinary open access archive for the deposit and dissemination of scientific research documents, whether they are published or not. The documents may come from teaching and research institutions in France or abroad, or from public or private research centers.

L'archive ouverte pluridisciplinaire **HAL**, est destinée au dépôt et à la diffusion de documents scientifiques de niveau recherche, publiés ou non, émanant des établissements d'enseignement et de recherche français ou étrangers, des laboratoires publics ou privés.



HAL Authorization

Highly efficient near-infrared quantum cutting in $\text{Ce}^{3+}/\text{Yb}^{3+}$ co-doped chalcohalide glasses

Bing Gao¹, Qiqi Yan¹, Yu Tong^{1,2}, Xianghua Zhang², Hongli Ma², Jean-luc Adam², Jing Ren¹,

Guorong Chen^{1*}

1. Key Laboratory for Ultrafine Materials of Ministry of Education, School of Materials Science and Engineering, East China University of Science and Technology, Shanghai 200237, China

2. Laboratoire des Verres et Céramiques, UMR-CNRS 6226, Sciences chimiques de Rennes, Université de Rennes 1, Rennes, 35042, France

Abstract

Near-infrared (NIR) quantum cutting involving the emission of two NIR photons for each visible photon absorbed is realized from $\text{Ce}^{3+}/\text{Yb}^{3+}$ codoped chalcohalide glasses. Excitation, emission and decay spectra are measured to prove the occurrence of energy transfer (ET) from Ce^{3+} to Yb^{3+} . The maximum ET efficiency obtained is as high as 82%, and the possible mechanism of ET is discussed. The directly measured and calculated quantum yield (QY) of the Yb^{3+} emission upon the excitation of $5d$ level of Ce^{3+} is up to 119%.

Key words: energy transfer; quantum cutting; chalcohalide glasses; Ce^{3+} ; Yb^{3+}

1.Introduction

Photovoltaics (PV) is an advanced technique that can directly convert clear and sustainable solar energy into electricity. Currently, PV devices fabricated from silicon (Si) wafers dominate the marketplace. Unfortunately, silicon based PV products are expensive and show poor efficiency when converting solar energy to electricity [1-3]. In order for PVs to play a major role in future energy generation it is necessary that the efficiency of these systems is improved. At present, the mismatch

* Corresponding author: grchen@ecust.edu.cn

between the solar photon flux spectrum and the spectral response of Si solar cells accounting for ~70% energy loss is one of the main factors limiting the efficiency of Si solar cells [4]. Downconversions including downshifting and quantum cutting (QC), are important methods of modifying the solar photon flux spectrum. Many efforts have been made to develop NIR QC phosphors or glasses co-doped with Yb^{3+} and other rare-earth ions (RE^{3+}) [5-7]. The Yb^{3+} is suitable as an acceptor and emitter because luminescence quantum efficiency of Yb^{3+} is close to 100% and most importantly, the transition energy from the only excited level to the ground state of Yb^{3+} : $^2\text{F}_{5/2} \rightarrow ^2\text{F}_{7/2}$ (~1.2 eV) is roughly in accordance with the band gap of Si (~1.1 eV). On the other hand, Ce^{3+} is different from other trivalent RE^{3+} owing to its unique electronic configuration. The absorption of Ce^{3+} originates from the allowed electric-dipole transition from the $4f$ ground state to the $5d$ excited one, which results in a very high absorption cross section on the order of 10^{-18} cm^2 [8]. Our previous work has shown that upon the blue (450 nm) excitation Ce^{3+} doped chalcogenide glasses emit 520 nm (~2.4 eV) photons [9, 10], which are exactly two times of the Yb^{3+} : $^2\text{F}_{5/2} \rightarrow ^2\text{F}_{7/2}$ transition. Moreover, chalcogenide glasses have been demonstrated to be good candidate for hosting RE^{3+} to obtain high ET efficiency and QY because of their low phonon energy (~350 cm^{-1}) [11]. In this paper, we demonstrate the highly efficient QC in the $\text{Ce}^{3+}/\text{Yb}^{3+}$ co-doped $\text{GeS}_2\text{-Ga}_2\text{S}_3\text{-CsCl}$ chalcogenide glasses involving the emission of two NIR photons of Yb^{3+} for each blue photon of Ce^{3+} absorbed via ET process.

2. Experiment

High-purity elements germanium (99.999%), gallium (99.999%), sulfur (99.999%), Cerium(99.999%), and ytterbium(99.999%) and compounds CsCl (99.9%) were loaded into a 10 mm inner-diameter silica tube and evacuated to a high vacuum level (10^{-3} Pa). The mixes were heated at 900 °C for 12 hours in a rocking furnace, and then quenched in the water. The glasses obtained were annealed at a temperature

20 °C below the glass transition temperature for 2 hours and then slowly cooled down to room temperature. The glass samples were cut into circular discs of 2 mm thickness and polished to optical quality using the superfine Al₂O₃ powders. The X-ray diffraction patterns confirmed that the prepared glasses were amorphous. The glass compositions are listed in Table I.

Absorption spectra were recorded by a Jasco V-570 spectrophotometer (Jasco International Co. Ltd., Tokyo, Japan). The excitation, emission spectra were collected by a high-resolution spectrofluorometer (Fluorolog-3, Horiba Jobin Yvon Inc., Edison, NJ) using a 450 W Xe-lamp as the excitation source. The decay curves of Ce³⁺ emission was performed by FLSP920 (Edinburgh Instruments). All measurements were carried out at room temperature.

To obtain the QY, a barium sulfate coated integrating sphere (150 mm in diameter) was attached to the FLS920. The blank laser excitation line from 440 to 460 nm was measured first. Then, the sample was placed on the sample holder in the integrating sphere for measurement of the emission spectra with Hamamatsu R928 and liquid-nitrogen-cooled Hamamatsu R5509-72 photomultiplier tubes in the NIR ranges. To eliminate the noise, every spectrum was scanned at least 5 times.

3. Results and Discussion

Fig.1 presents normalized absorption spectra of glass samples G1-G5. The absorption cut-off edge of the G1 glass is located at 450 nm. The absorption band of the $^2F_{5/2} \rightarrow ^2F_{7/2}$ transition of Yb³⁺ ranging from 900 nm to 1100 nm can be clearly identified from the inset figure which is enlarged from 900 nm to 1050 nm. Apparently, the absorbance around 980 nm increases with increasing Yb³⁺ concentration.

Fig. 2 shows the emission and excitation spectra of the Yb³⁺ single doped (G0), Ce³⁺ single doped (G1) and Ce³⁺/Yb³⁺ codoped (G2) samples. Under the excitation of 450 nm, the Yb³⁺ single doped sample shows no emission in both visible and NIR regions. The Ce³⁺ single doped sample, on the other hand,

exhibits an intense blue emission band centered at 520 nm. The emission is due to the $d-f$ [$^4f_0^5d_1 \rightarrow ^4f_1(^2F_J)$] transition of Ce^{3+} ion from $5d$ excited state to $2F$ ground state, which is a parity allowed electric dipole (e-d) transition with large oscillator strength [9,10]. Compared to the single doped samples, the codoped sample shows very strong NIR emissions centered at ~ 980 nm-1020 nm due to the $^2F_{5/2} \rightarrow ^2F_{7/2}$ transitions of Yb^{3+} [5-7], but the visible emission is much reduced, implying that there exists an efficient ET from Ce^{3+} to Yb^{3+} . From the excitation spectra monitored at the 988 nm emission of Yb^{3+} (dashed line in Fig.2) it is clear that co-doping of Ce^{3+} (G2) leads to a much broader and more intense excitation band with the maximum wavelength shifted to the blue region. The greatly increased excitation cross-section (ECS, the area under the excitation band) of the codoped sample is benefiting energy harvesting of light sources [11].

Fig. 3 shows the visible and NIR emission spectra of the samples with fixed Ce^{3+} but varying Yb^{3+} concentrations (G1-G5). With the increasing Yb^{3+} concentration, the yellow-green emission of Ce^{3+} gradually decreases until almost totally quenched in the highest Yb^{3+} concentration (G5). Concomitantly, the broad NIR emissions band around 1000 nm from Yb^{3+} : $^2F_{5/2} \rightarrow ^2F_{7/2}$ transition are enhanced greatly until the Yb^{3+} concentration reaches 0.6 mol% due to concentration quenching effect (G5). The above phenomenon is also a direct evidence of ET from Ce^{3+} to Yb^{3+} .

To better understand the ET between Ce^{3+} and Yb^{3+} and the high ET efficiency, it is important to study the ET mechanism. The energy mismatch between one photon from Ce^{3+} ion ($\sim 19300 \text{ cm}^{-1}$) and the sum of two photons from Yb^{3+} ion ($\sim 20000 \text{ cm}^{-1}$) is $\sim 700 \text{ cm}^{-1}$, which almost equals to two times of the phonon energy of the current glass [11]. Thus the ET between Ce^{3+} and Yb^{3+} is assisted by two phonons. The electronic transitions which may be involved in the phonon-assisted ET (PAET) process between Ce^{3+} and Yb^{3+} ions are depicted in Fig.4. The PAET process proceeds via the following way:

upon the 450 nm excitation, Ce^{3+} ions emit at 520 nm due to the $\text{Ce}^{3+}: {}^4f_0^5d_1 \rightarrow {}^4f_1({}^2F_1)$ transition, the energies of the emitted photons together with two phonons from the glass matrix are simultaneously absorbed by two nearby Yb^{3+} ions. As a result, two NIR photons are generated due to the $\text{Yb}^{3+}: {}^2F_{5/2} \rightarrow {}^2F_{7/2}$ transition.

It is known that the ET efficiency (η_T) between sensitizer (Ce^{3+}) and activator (Yb^{3+}) can be expressed by the empirical equation: $\eta_T = 1 - \tau_s / \tau_{s0}$, where τ_s and τ_{s0} are the decay lifetimes of the sensitizer (Ce^{3+}) with and without the activator (Yb^{3+}), respectively [12]. Fig.5 presents photoluminescence decay of the Ce^{3+} 520 nm emission for G1-G5 samples. The decay times of Ce^{3+} in the single doped (G1) and codoped samples (G2, G3, G4, G5) are listed in the inset table. From the table it is seen that the decay time decreases with the increasing concentration of Yb^{3+} ions while the ET efficiency increases steadily up to about 82% (G5). However, this value is obtained by considering only the ion-ion interaction and should be regarded as the upper limit of ET efficiency.

The fluorescence quantum yield (QY, defined as η) can be ideally calculated with the measured life time of Ce^{3+} from the following equation:

$$\eta = 2\eta_{Yb}\eta_T$$

where η_{Yb} is the emission quantum efficiency of Yb^{3+} , usually about 100% because of the very low multiphonon relaxation rate due to the large energy gap to the next lower level, the ground state; η_T is the energy transfer efficiency [13]. Thus we can get the calculated QY equals to 104%, 136%, 156%, 164% for G2-G5, respectively.

Actually, QY is defined as the probability for a sample to emit a photon through fluorescence when it is excited by a single photon. It is therefore also the percentage of photons emitted by a bulk sample when a given number of photons are absorbed by the sample, i.e., the number of photons emitted divided by

the number of photons absorbed by a sample. The number of photons absorbed by a bulk sample is equal to the number of photons incident minus the photons passing through and not being absorbed. From this definition, QY can be measured by using an integrating sphere and calculated according to the following equation:

$$\eta = \int L_S / (\int E_R - \int E_S)$$

where, L_S is the NIR luminescence emission spectrum of the sample; E_S is the spectrum of the light used for exciting the sample and E_R is the spectrum of the excitation light without the sample in the sphere. As an illustration, the excitation lines of the G2 sample are shown in Fig.6 with all measured QYs listed in the inset table. With the increasing concentration of Yb^{3+} , the QY increases until G5 where the concentration quenching effect occurs. To maximize the luminescence output of the Yb^{3+} ions, one has to consider competition between the energy-transfer efficiency increasing the Yb^{3+} emission intensity for higher Yb^{3+} concentration and concentration quenching decreasing the Yb^{3+} luminescence intensity for higher Yb^{3+} concentration[14]. The obtained maximum QY is 119%, which is lower than the calculated value from the decay lifetime, but it is higher than $\text{Ce}^{3+}\text{-Yb}^{3+}$ co-doped $\text{Y}_3\text{Al}_5\text{O}_{12}$ (YAG) ceramics [13,15].

4. Conclusions

Quantum cutting (QC) of one visible photon into two NIR photons is realized in $\text{Ce}^{3+}/\text{Yb}^{3+}$ codoped chalcogenide glasses by phonon-assisted energy transfer (PAET) from Ce^{3+} to Yb^{3+} . The much enhanced Yb^{3+} emission and the high ET efficiency (82%) are probably because of the significantly increased ECS at the visible region. The maximum measured quantum yields of Yb^{3+} emission upon the $\text{Ce}^{3+}:5d$ level excitation is up to 119%, lower than that calculated from decay lifetime of Ce^{3+} . Our work shows an effective way for the realization of efficient spectral modification of the solar spectrum

in the applications of Si based solar cells.

5. Acknowledgements

This study was supported by Shanghai Leading Academic Discipline Project (No. B502), Shanghai Key Laboratory Project (08DZ2230500), Research Funds for Young Teachers for the Doctoral Program by Ministry of Education of China (20110074120022) and the National Natural Science Foundation of China (NSFC 51072052). Erreur ! Source du renvoi introuvable.

References

- [1] B. van der Zwaan, A. Rabl, Sol. Energy. 74 (2003) 19-31.
- [2] B. Richards, S. Sol. Energy Mater. Sol. Cells. 90 (2006) 2329-2337.
- [3] M. Y. Peng, L. J. Wondraczek, Mater. Chem. 19 (2009) 627-630.
- [4] Y. Teng, J. Zhou, X. Liu, S. Ye, J. Qiu, Opt. Express. 18,9 (2010) 9671-9676.
- [5] B. M. van der Ende, L. Aarts, A. Meijerink, Adv.Mater. 21,30 (2009) 3073-3077.
- [6] Q. Zhang, G. Yang, Z. Jiang, Appl. Phys. Lett. 91,5 (2007) 051903:1-3.
- [7] J. Zhou, Y. Zhuang, S.Ye, Y. Teng, G. Lin, B. Zhu, J. Xie, J. Qiu, Appl. Phys. Lett. 95, 141 (2009) 101:1-3.
- [8] D. Chen, Y. Wang, Y. Yu, P. Huang, F. Weng, J.Appl. Phys. 104,116 (2008) 105: 1-3.
- [9] Q. Yan, C. Shen, W. Wang, G. Chen, J. Alloys Compd. 508, 2 (2010) L24-L27.
- [10] C. Shen, Q. Yan, Y. Xu, G. Yang, S.Wang, Z. Xing, G. Chen, J. Am. Ceram. Soc.93,3 (2010) 614-617.
- [11] Q. Yan, J. Ren, G. Chen, J. Am. Ceram. Soc. (2012) 1-3.
- [12] W.-J. Yang, L. Luo, T.-M. Chen, N.-S. Wang, Chem. Mater. 17,15 (2005) 3883-3888.
- [13] J. Ueda, S. Tanabe, J. Appl. Phys. 106, 043101 (2009) 1-3.
- [14] P. Vergeer, T. J. H. Vlugt, M. H. F. Kox, M. I. den Hertog, J. P. J. M. van der Eerden, and A. Meijerink, Phys. Rev. B. 71, 014119 (2005)
- [15] Y. Xu, X. Zhang, S. Dai, B. Fan, H. Ma, J. Adam, J. Ren, G. Chen, J. Phys. Chem. C. 115 (2011) 13056–13062.

Figure Captions

Table I Nominal compositions (mol.%) of glass samples.

Fig.1 Normalized absorption spectra of the G1-G5 glass samples.

Fig.2 Emission spectra of the Yb³⁺ single doped (G0), Ce³⁺ single doped (G1) and Ce³⁺/Yb³⁺ codoped (G2) samples upon the excitation of 450 nm light (solid line); Excitation spectra of the G0 and G2 samples monitored at 988 nm emission (dashed line).

Fig.3 Visible and NIR emission spectra of the samples with fixed concentration of Ce³⁺ but varying concentration of Yb³⁺ (G1-G5). The excitation wavelength is 450 nm.

Fig.4 Energy level diagrams of Ce³⁺ and Yb³⁺ and possible ET process between Ce³⁺ and Yb³⁺.

Fig.5 Photoluminescence decay of the Ce³⁺ 520 nm emission for the G1-G5 samples. The inset table shows the decay times and energy transfer efficiencies.

Fig.6 Excitation line of the G2 sample collected by using an integrating sphere. The inset table is the quantum yield of the sample in NIR.

Table I Nominal compositions (mol.%) of glass samples.

Samples	G0	G1	G2	G3	G4	G5
Host glass	50GeS ₂ -25Ga ₂ S ₃ -25CsCl					
Ce ³⁺	0	0.08	0.08	0.08	0.08	0.08
Yb ³⁺	0.1	0	0.1	0.25	0.5	0.6

Fig. 1

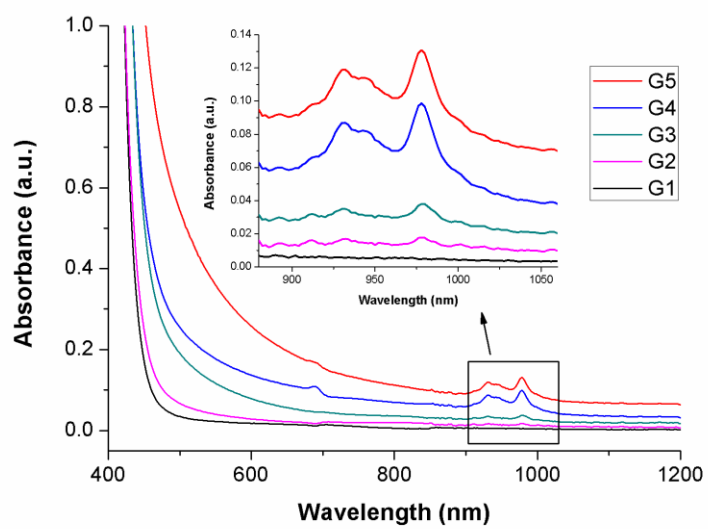


Fig. 2

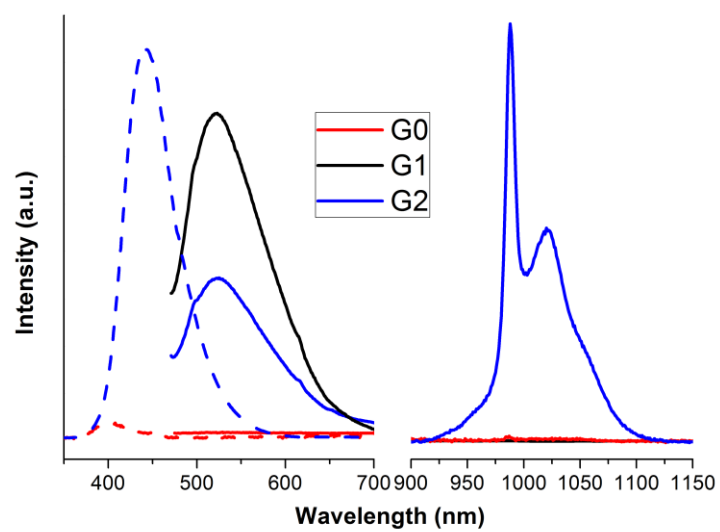


Fig. 3

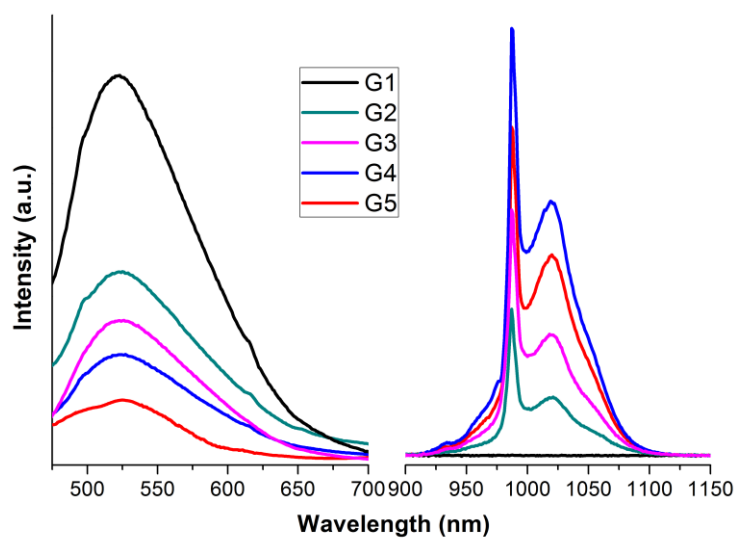


Fig. 4

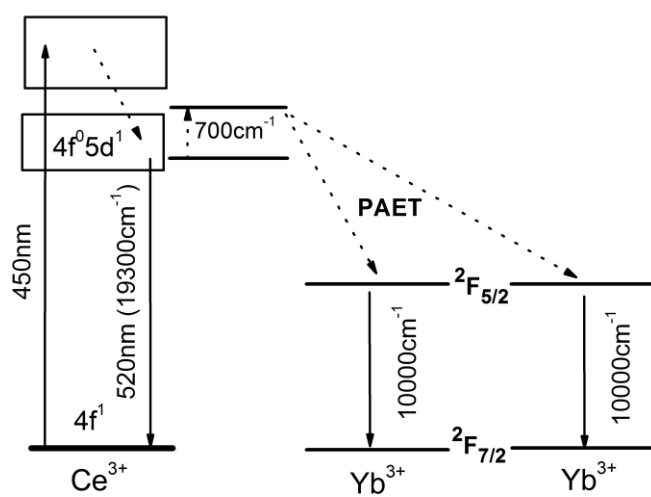


Fig.5

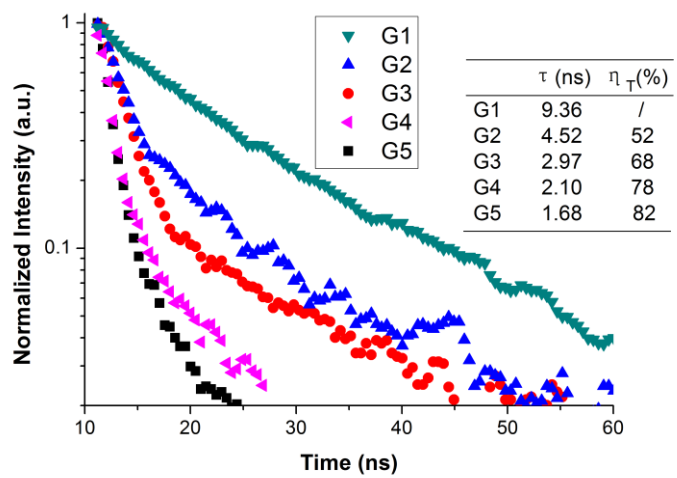


Fig. 6

